

## MECHANICAL BEHAVIOR IN COMPRESSION AND FLEXURE OF BIOACTIVE GLASS (13-93) SCAFFOLDS PREPARED BY ROBOTIC DEPOSITION

Xin Liu<sup>1,2</sup>, Mohamed N. Rahaman<sup>1,2</sup>, Greg E. Hilmas<sup>1</sup>

<sup>1</sup>Department of Materials Science and Engineering; <sup>2</sup>Center for Bone and Tissue Repair and Regeneration, Missouri University of Science and Technology, Rolla, Missouri 65409

### ABSTRACT

There is a need to develop synthetic scaffolds for repairing large defects in load-bearing bones. Our recent work has shown the ability to create strong porous scaffolds of bioactive glass with a grid-like microstructure by robotic deposition (robocasting) which have compressive strengths comparable to cortical bone. In the present work, the mechanical properties of those 13-93 bioactive glass scaffolds were evaluated in compressive and flexural loading to determine their strength, elastic modulus, and Weibull modulus. The scaffolds had a porosity of ~50%, a glass filament diameter of ~300  $\mu\text{m}$ , and a pore width of ~300  $\mu\text{m}$  in the plane of deposition (xy plane) and ~150  $\mu\text{m}$  in z direction. The load in both testing modes was applied in the z direction, and the scaffolds were tested as-fabricated and after immersion in a simulated body fluid (SBF) in vitro. As fabricated, the scaffolds had a strength =  $86 \pm 9$  MPa, elastic modulus =  $13 \pm 2$  GPa, and Weibull modulus = 12 in compression. The strength, elastic modulus, and Weibull modulus in flexure were  $11 \pm 3$  MPa,  $13 \pm 2$  GPa, and 6, respectively. The compressive strength and elastic modulus decreased markedly during the first 2 weeks of immersion in SBF, but more slowly thereafter. The consequences of these results for the potential application of this type of bioactive glass scaffold in the regeneration of loaded bone are discussed.

### INTRODUCTION

There is a clinical need for the development of synthetic scaffolds to repair large bone defects resulting from trauma, resection of tumors, and congenital diseases. There were approximately 1.6 million bone graft procedures performed in the United States in 2005 alone, and a significant fraction of those was used to treat bone defects in the elderly [1]. As the population ages and life expectancy continues to rise, the number of bone graft procedures is expected to increase substantially. Traditionally, bone allograft, metal spacers, and even bone cement have been used to restore large bone defects, such as segmental defects in the limbs. However, these methods are limited by high costs, limited availability, unpredictable long-term durability, and uncertain healing to host bone. Synthetic biocompatible porous 3D scaffolds that replicate the structure and function of bone would be ideal bone substitutes, provided they have the requisite mechanical properties for reliable long-term cyclical loading during weight bearing.

Ideally, scaffolds for bone regeneration should be biocompatible and biodegradable, with a three-dimensional (3D) architecture of interconnected pores capable of supporting new bone growth [2]. For the regeneration of load-bearing bones, the mechanical properties of the scaffolds are also important, but there are no clear guidelines on the target mechanical properties. It has often been stated that the mechanical properties of the scaffold should be comparable to those of the bone to be replaced.

Bioactive glass, as a scaffold material, has several attractive properties. When placed in the body fluid, bioactive glass reacts to form a layer of hydroxyapatite (HA)-like material (the main mineral constituent of bone) on the surface of the glass, which is responsible for the formation of a strong bond with hard and soft tissues [2, 3]. Bioactive glass is biocompatible, heal to host bone, degrade into non-toxic products, and can be fabricated into porous 3D configurations. For similar microstructures, bioactive glass has the potential to provide scaffolds with higher mechanical strength when compared to polymers. Recent studies have shown that silicate 13-93 and 6P53B bioactive glass

scaffolds with a grid-like microstructure, prepared by robocasting, a solid freeform fabrication (SFF) technique, have compressive strengths comparable to those reported for human cortical bone [4-6].

Although the mechanical properties of bioactive glass scaffolds have been widely reported in the literature, most studies have focused mainly on the compressive strength and elastic modulus of the scaffolds, as-fabricated or after immersion in an aqueous phosphate solution such as simulated body fluid (SBF) [7, 8]. The design of bioactive glass scaffolds for regenerating large defects in load-bearing bones requires additional information on the mechanical response, such as strength and elastic modulus in multiple loading modes (compression; flexure; torsion), mechanical reliability (Weibull modulus), fatigue resistance, and fracture toughness. In addition, the mechanical response of the scaffolds in vitro, as a function of immersion time in SBF, and in vivo, after implantation in animal models, is also important.

Our long-term objective is to comprehensively characterize the mechanical properties of bioactive glass scaffolds prepared by robocasting in vitro and after implantation in vivo in suitable animal models. In the present manuscript, the mechanical properties of silicate 13-93 bioactive glass scaffolds in compression and in flexure are described. The strength, elastic modulus, and Weibull modulus of 13-93 bioactive glass scaffolds with a grid-like microstructure were measured and analyzed. The scaffolds were tested as-fabricated, and as a function of immersion time in SBF.

### METHODS

#### Fabrication of 13-93 bioactive glass scaffolds by robocasting

Melt-derived bioactive glass frits with the 13-93 composition (wt%):  $53\text{SiO}_2$ ,  $6\text{Na}_2\text{O}$ ,  $12\text{K}_2\text{O}$ ,  $5\text{MgO}$ ,  $20\text{CaO}$ ,  $4\text{P}_2\text{O}_5$ , provided by Mo-Sci Corp., Rolla, MO, USA, were ground in a SPEX mill, and then attrition-milled for 2 h in water with  $\text{ZrO}_2$  grinding media to produce particles of size  $\sim 1\ \mu\text{m}$ . The preparation of an ink for deposition of the scaffolds by robocasting is described in detail elsewhere [6]. Briefly, the glass particles (40 vol %) were mixed with a 20 wt % aqueous Pluronic® F-127 solution which was pre-cooled in the refrigerator using a planetary centrifugal mixer (ARE-310, THINKY U.S.A. Inc, Laguna Hills, CA) and placed at  $10\ ^\circ\text{C}$  in a refrigerator for 12 h. The ink was brought up to room temperature ( $\sim 25\ ^\circ\text{C}$ ), loaded into a robocasting machine (RoboCAD 3.0, 3-D Inks, Stillwater, OK, USA) and printed on an  $\text{Al}_2\text{O}_3$  substrate immersed in a reservoir of lamp oil (Florasense, Chaleston, SC). The ink was extruded through a nozzle of diameter  $410\ \mu\text{m}$ . The spacing between the centers of adjacent filaments was set at  $910\ \mu\text{m}$ . After deposition, the scaffolds were dried for 24 h in air, heated slowly ( $0.5\ ^\circ\text{C}/\text{min}$  with a few isothermal holds) to  $600\ ^\circ\text{C}$  in flowing  $\text{O}_2$  gas to burn out the organic processing additives, and sintered in air for 1 h at  $700\ ^\circ\text{C}$  (heating rate =  $5\ ^\circ\text{C}/\text{min}$ ) to densify the glass filaments.

The as-fabricated scaffolds were coated with Au/Pd, and examined in a scanning electron microscope (SEM) (S-4700; Hitachi, Tokyo, Japan) at an accelerating voltage of 15 kV and a working distance of 12 mm. The pore width and glass filament diameter were measured using Image J software, and the interconnected porosity was measured using the Archimedes method.

#### Mechanical testing

Samples for mechanical testing in compression were prepared by sectioning the as-fabricated 13-93 scaffolds using a diamond-coated blade, and grinding into a cubic shape ( $6\ \text{mm} \times 6\ \text{mm} \times 6\ \text{mm}$ ) using a surface grinder (FSG-618, Chevalier Machinery Inc., Santa Fe Springs, CA). The compressive strength of the scaffolds was measured at a cross-head speed of  $0.5\ \text{mm}\cdot\text{min}^{-1}$  along the z direction using an Instron testing machine (Model 5881; Norwood, MA, USA). The deformation of the sample was determined from the movement of the cross-head. The elastic modulus was determined from the slope of the linear region of the stress vs. strain response.

The strength and elastic modulus in flexure were measured by four-point bending of as-fabricated rectangular bars (3 mm × 5 mm × 25 mm) in a fully articulated fixture with an outer span = 20 mm and an inner span = 10 mm, at a crosshead speed of 0.2 mm min<sup>-1</sup>. Flexural testing was performed according to the procedure described in ASTM C1674-08. The stress was applied in the z direction of the scaffolds (the same direction used for the compression tests). The deflection during the test was measured continuously using a linear variable differential transformer (LVDT) at the mid-span of the sample, and used to determine the strain. The flexural strength was determined using the equation:

$$\sigma = \frac{3PL}{4bd^2} \quad (1)$$

where P is the applied load, L is the outer span of the fixture, and b and d are the width and thickness, respectively, of the sample. The elastic modulus was determined from the slope of the linear region of the flexural stress vs. strain curve. Thirty samples each were tested in compression and in flexure, and the results were determined as an average ± standard deviation.

The Weibull modulus of the bioactive glass scaffolds in compression and in flexure was determined from the strengths of the 30 samples tested in each loading mode. The analysis was performed according to the ASTM standard C 1239-07, from a plot of

$$\ln \ln \left( \frac{1}{1-P_f} \right) = m \ln \left( \frac{\sigma}{\sigma_0} \right) \quad (2)$$

where  $P_f$  is the probability of failure at a stress  $\sigma$ , and  $\sigma_0$  is the Weibull scale parameter determined from the intercept of the fit to the data and Weibull modulus,  $m$ . The value  $\sigma_0$  is also the stress at which the probability of failure is 63%.  $P_f$  was evaluated using the equation

$$P_f = \frac{i-0.5}{n} \quad (3)$$

where  $n$  is the total number of specimens tested and  $i$  is the specimen rank in ascending order of failure stresses.

#### Degradation of mechanical properties in vitro

The as-fabricated scaffolds with a cubic shape (similar to those used in the compression test) were immersed for selected times in SBF at 37 °C, and tested in compression using the method described previously. Six samples were tested for each immersion time, and the data were used to determine the compressive strength and elastic modulus as an average ± standard deviation.

After immersion in SBF (and prior to mechanical testing), the scaffolds were mounted in epoxy resin, sectioned, ground and polished to reveal the cross-sections of the converted glass filaments. The samples were coated with carbon and examined in an SEM (Hitachi S-4700) using the backscattered electron (BSE) mode at an accelerating voltage of 15 kV and a working distance of 13 mm. The SEM images were used to determine the thickness of the converted layer on the glass surface.

#### RESULTS AND DISCUSSION

The as-fabricated scaffolds (**Fig. 1a**) had a uniform grid-like microstructure, composed of almost fully dense glass filaments (~300 μm in diameter). The pore width in the plane of deposition (xy plane) was 300 ± 10 μm, while the pore width in the direction of deposition (z direction) was 150 ±

10  $\mu\text{m}$  (Fig. 1a; inset). The porosity of the scaffolds, as determined by the Archimedes method, was  $47 \pm 1\%$ .

The measured mechanical properties of the as-fabricated scaffolds are summarized in Table I. For comparison, the mechanical properties of human cortical and trabecular bones are also given. The elastic modulus in compression and the flexural modulus of the scaffolds were approximately the same ( $13 \pm 2$  GPa), in the range reported for cortical bone. For the same porosity, the compressive strength of the scaffolds ( $86 \pm 9$  MPa) was comparable to the highest strengths reported for bioactive glass scaffolds prepared by solid freeform fabrication techniques, and far higher than the strengths reported for bioactive glass scaffolds prepared by more conventional techniques [7]. While the flexural strength of the bioactive glass scaffolds was much lower than the flexural strength, the value ( $11 \pm 3$  MPa) was comparable to the highest values reported for hydroxyapatite scaffolds with similar porosity [8].

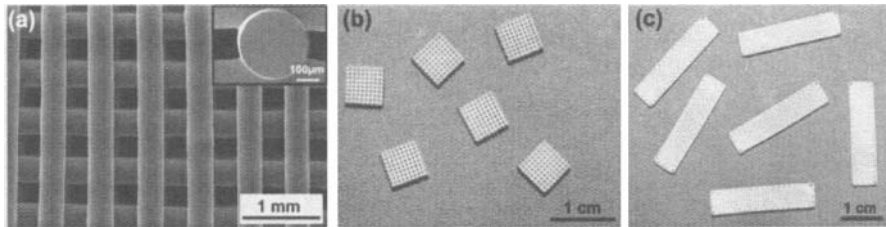


Figure 1. (a) SEM image showing the microstructure (in the xy plane) of the as-fabricated silicate 13-93 bioactive glass scaffolds prepared by robocasting (Inset: cross-section of the glass filament); (b), (c) optical images showing the xy plane of cubic samples used for mechanical testing in compression, and the xy plane of rectangular bars used for testing in flexure. The load was applied in the z direction (perpendicular to the xy plane shown) in both testing modes.

**Table I** Mechanical properties of the as-fabricated 13-93 bioactive glass scaffolds with grid-like microstructure; for comparison, the properties of human cortical bone and trabecular bone are also shown

	Compression			Flexure		
	Strength (MPa)	Weibull Modulus	Elastic modulus (GPa)	Strength (MPa)	Weibull Modulus	Flexural modulus (GPa)
Scaffolds	$86 \pm 9$	12	$13 \pm 2$	$11 \pm 3$	6	$13 \pm 2$
Cortical bone [7]	100–150		10–20	135–193		10–20
Trabecular bone [7]	2–12		0.1–5	10–20		0.1–5

In the present study, the samples were tested by applying the load in the z direction, to match the compressive loading of the scaffolds when implanted in segmental long bone defects. However, the mechanical properties of the scaffolds are expected to be anisotropic because of the different arrangement of the glass filaments in the xy plane and in the planed perpendicular to that plane (Fig. 1a). Scaffolds are currently being tested to measure the compressive and flexural strengths in the x (or, equivalently, the y direction). In the literature, scaffolds of silicate 6P53B bioactive glass with a grid-like microstructure (pore width of  $500 \mu\text{m}$  in the the xy plane and  $<50 \mu\text{m}$  in the z direction) showed a

compressive strength in the z direction which was  $\sim 1.5$  times higher than the value in the x or y direction [6]. Scaffolds of hydroxyapatite (HA) and beta-tricalcium phosphate ( $\beta$ -TCP), pore width of  $80\ \mu\text{m}$  in xy plane and  $120\ \mu\text{m}$  in z direction, showed a slightly lower compressive strength when tested in the z direction than in the x (or y) direction, in accordance with the predictions of finite element analysis [9].

**Figure 2** shows Weibull plots of the measured compressive and flexural strengths for the 13-93 bioactive glass scaffolds with a grid-like microstructure. The Weibull modulus (slope of the plot) determined from the data for a large number of samples (typically more than 20–30) is commonly used as a measure of the mechanical reliability of the samples or the probability of failure. Together with the strength, the Weibull modulus is used to evaluate the safety (probability of failure) of a brittle material under a given stress. However, data on the Weibull modulus of bioactive glass scaffolds are limited. The mechanical response of brittle materials such as glass and ceramics are sensitive to cracks and defects. Dense glass and ceramics have been reported to have a Weibull modulus in the range 5 to 20 [10]. In comparison, the Weibull modulus of porous calcium phosphate bioceramic scaffolds, such as hydroxyapatite,  $\beta$ -tricalcium phosphate, and biphasic calcium phosphate tested in compression, has been reported in the range 3 to 10 [11–13]. In the present study, the Weibull modulus of the bioactive glass scaffolds in compression was 12 (**Fig. 2**). Under the same allowable failure probability,  $P_f = 10^{-3}$ , the bioactive glass scaffolds prepared in this study showed a failure strength of 50 MPa in compression, which was higher than the values for calcium phosphate bioceramic scaffolds with similar porosity (**Fig. 2**).

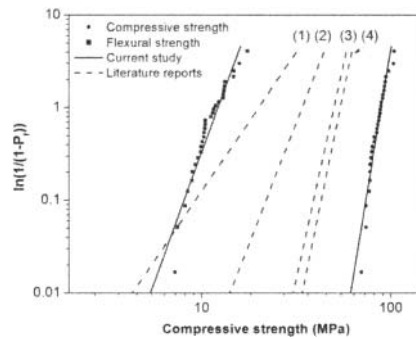


Figure 2. Weibull plots of the compressive and flexural strength data from the present study. For comparison, Weibull plots of the compressive strength data from the literature are also shown (dashed lines): (1)  $\beta$ -tricalcium phosphate scaffolds fabricated by robocasting [11]; (2, 3) oriented calcium polyphosphate scaffolds prepared by solid freeform fabrication tested in the strong and weak directions, respectively [12]; (4) hydroxyapatite scaffolds fabricated by robocasting [13].

The flexural strength and Weibull modulus of the scaffolds fabricated in the present study (porosity  $\sim 50\%$ ) are  $11 \pm 3$  MPa and 6, respectively. In comparison, the flexural strengths of porous calcium phosphate bioceramics are in the range 2 to 12 MPa for scaffolds with porosity of 30–50% [8]. These flexural strengths are all much lower than the values for human cortical bone (135–190 MPa), and only in the range of values for trabecular bone (**Table I**). Improvement in the flexural strength of the scaffolds requires alternative designs aimed at strengthening the regions of the scaffold susceptible to tensile stresses during flexure. Another approach which has been used to improve the compressive strength of calcium phosphate bioceramic scaffolds is the infiltration of the pores with a biodegradable

polymer [11]. However, infiltrating or coating bioactive glass scaffolds with a biodegradable polymer will reduce the interactions between cells and the bioactive glass surface.

Finite element analysis of a grid-like microstructure showed that the magnitude and distribution of stress generated within the scaffold under compressive loading was very different from that under tensile loading [9]. Under the same load, the maximum local tensile stress generated in the glass filaments as a result of tensile loading was much higher than that in compressive loading. Since brittle materials such as glass typically fail in tension, and assuming that the scaffolds failed when the maximum local tensile stress exceeded the tensile strength of the glass filament, then the compressive strength will be far superior to with tensile strength [9]. The results of the current studies, which showed that the flexural strength was much lower than the tensile strength, are in general agreement with the predictions of the finite element modeling.

The strength and Weibull modulus of porous glass and ceramics depend on both the distribution of the flaws in the solid phase and the on size and size distribution of the pore phase. In the present study, the bioactive glass filaments in the scaffolds were sintered to almost full density (Fig. 1a), which had the effect of reducing the size and number of flaws in the glass phase. The dense glass filaments and the well-controlled porous architecture resulting from the use of computer-aided design and the robocasting method presumably contributed to the high compressive strength and Weibull modulus found in the present work.

#### Degradation of the mechanical strength in vitro

In compression, the scaffolds, as-fabricated or immersed for various times in SBF, showed an elastic response followed by brittle failure (Fig. 3). The compressive strength of the scaffolds as a function of immersion time in SBF in vitro is shown in Fig 4a. A large decrease in strength occurred during the first two weeks; the strength decreased from  $86 \pm 9$  MPa for the as-fabricated scaffold to  $58 \pm 5$  MPa after the two-week immersion (~67% of the as-fabricated strength). Thereafter, the compressive strength decreased more slowly. This trend in the strength degradation is similar to that found in a recent study [6] for scaffolds of another silicate bioactive glass (6P53B) prepared by robocasting. In that study, the strength of the scaffolds dropped sharply to ~60% of the as-fabricated value upon immersion in SBF, but then decreased more slowly at longer times [6]. The change in the elastic modulus of the scaffolds measured in compression followed a trend similar to that of the compressive strength; a large decrease initially was followed by a slower rate of decrease (Fig. 4b).

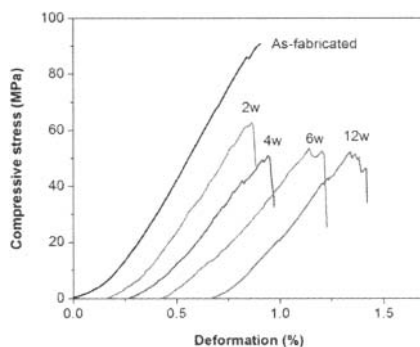


Figure 3. Mechanical response in compression of 13-93 bioactive glass scaffolds as a function of immersion time (in weeks) in SBF. (The curves were shifted along the x-axis to maintain clarity.)

## Mechanical Behavior in Compression and Flexure of Bioactive Glass (13-93) Scaffolds

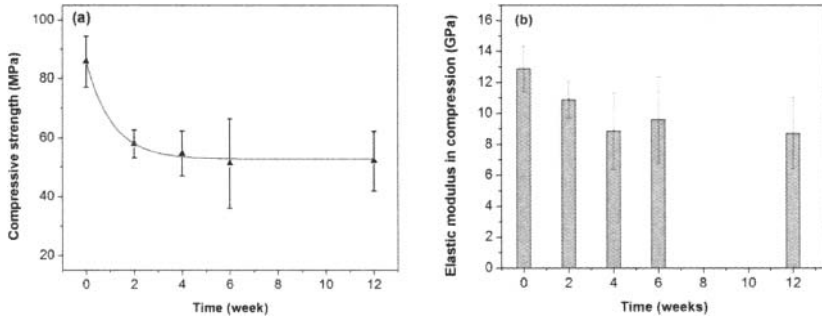


Figure 4. (a) Strength and (b) elastic modulus of 13-93 bioactive glass scaffolds in compression as a function of immersion time in SBF *in vitro*.

SEM images of the cross-section of the glass filaments (**Fig. 5**) in the scaffolds showed that after 6 weeks immersion in SBF, a thin layer of the glass surface was converted to an HA-like material. The thickness of the converted layer ( $\sim 5 \mu\text{m}$ ) was smaller than the values observed for the same 13-93 bioactive glass *in vivo*. When implanted for 6–12 weeks in rat calvarial defects and in rat subcutaneous sites, the thickness of the converted layer was 20–30  $\mu\text{m}$  [14, 15]. The faster conversion of glass *in vivo* was presumably due to the more dynamic environment in the body as well as the presence of electrolytes, proteins and biological polymers in the body fluid [16, 17]. Although the SBF was stirred periodically, *in vitro* immersion conditions were less dynamic and the volume of the SBF was constant. Because of the faster conversion of the glass *in vivo*, it is expected that the mechanical strength of the scaffold would degrade faster *in vivo* than *in vitro*. Current work is aimed at measuring the strength of similar bioactive glass scaffolds as a function of implantation time in animal models.

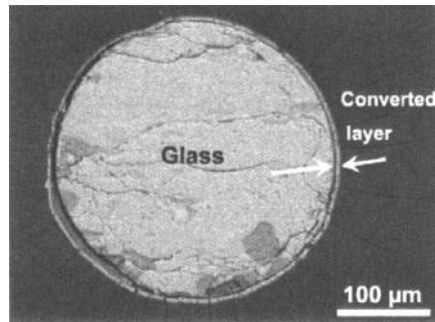


Figure 5. SEM backscattered electron image showing the cross-sections of the glass filament of 13-93 bioactive glass scaffolds after immersion in simulated body for 6 weeks.

### Bioactive glass scaffolds for load-bearing bone repair

The regeneration of large defects in loaded bone using bioactive glass scaffolds depends on a

combination of factors, such as the conversion rate of the bioactive glass to HA, the degradation of the mechanical properties of the scaffold with time, the rate of bone ingrowth into the scaffold, and the ability of the converted HA material to remodel into bone. A challenge in designing bioactive scaffolds for the regeneration of loaded bone is in matching the conversion rate of the glass to HA and consequent degradation in mechanical properties with the rate of new bone growth. Low as-fabricated strength as well as rapid degradation in strength *in vivo* would limit the ability of the scaffolds to support physiological loads. As illustrated in Fig. 6, the repair of loaded bone defects can be divided into two stages. In the first stage, the ability to support physiological loads is provided mainly by the scaffold itself, whereas in the second stage, infiltration of new bone into the scaffold should contribute to a much greater extent to the strength of the implant. The transition from the first stage to the second stage is currently unclear but it is presumably in the range 6–12 weeks for clinically relevant applications.

The high compressive strength and high Weibull modulus of the 13-93 bioactive glass scaffolds prepared in this study are favorable for the survival of the implants early after surgery. Other aids, such as commercially available fixation devices and supporting systems for bone defect treatment, are also used to share the load and limit the peak loads from acting on the implants to prevent failure early after surgery. However, mechanical loading on the bone graft is still required for bone regeneration and remodeling in later stage in order to avoid stress shielding, a possible cause of bone loss. Therefore, it is necessary to optimize and predict the mechanical strength of the implants during the bone regeneration progress.

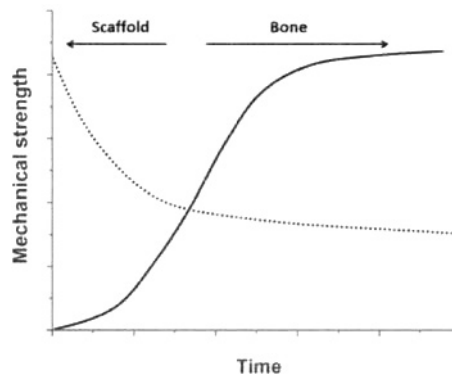


Figure 6. Schematic diagram illustrating trends in the strength of bioactive glass scaffolds and new bone formation *in vivo* as a function of implantation time. The cross-over point between the two curves is arbitrary. In the first region (shorter implantation time), the scaffold provides the main load-bearing capability, while in the second region (longer implantation time), new bone formed in the scaffold should provide an increasing contribution to the implant strength.

Attempts have been made to predict the mechanical strength of biodegradable polymer scaffolds by computational simulation based on the known degradation mechanism and bone formation rate [18]. In the case of bioactive glass scaffolds, data for the change in mechanical properties as a function of implantation time *in vivo* is currently limited. This present study showed that the early stage (< 2–4 weeks) is crucial for the survival of the bioactive glass scaffold implants, because of the rapid degradation in mechanical properties. In addition, the amount of new bone formed in that time is expected to be small [18]. Our current work is aimed at characterizing the mechanical properties of



porous strong bioactive glass scaffolds in multiple loading modes in vitro and in vivo, and evaluation of the scaffold in osseous defects in animal models.

## CONCLUSIONS

Scaffolds of 13-93 bioactive glass prepared with a grid-like microstructure by robocasting (porosity ~50%; glass filament width ~300  $\mu\text{m}$ ; pore width ~300 in the xy plane and ~150  $\mu\text{m}$  in z direction) had a strength of  $86 \pm 9$  MPa, elastic modulus of  $13 \pm 2$  GPa, and a Weibull modulus of 12 when tested in compression in the z direction. In flexural loading in the z direction, the strength, elastic modulus, and Weibull modulus were  $11 \pm 3$  MPa, and  $13 \pm 2$  GPa, and 6, respectively. Upon immersion of the scaffolds in simulated body fluid, the compressive strength and elastic modulus decreased rapidly during the first two weeks, to ~67% of the as-fabricated values. Thereafter, the strength and elastic modulus decreased more slowly with immersion time. The compressive mechanical properties of the scaffolds are promising for loaded bone repair. However, further work is needed to optimize the mechanical properties of the scaffolds in multiple loading modes and to evaluate their capacity to support bone regeneration in osseous defects in animal models.

## ACKNOWLEDGEMENTS

This work was supported by the National Institutes of Health, National Institute of Arthritis, Musculoskeletal and Skin Diseases (NIAMS), Grant # 1R15AR056119-01. The authors thank Mo-Sci Corp., Rolla, MO for the bioactive glass used in this work, and Dr. Jeremy Watts for assistance with designing a fixture for flexural tests.

## REFERENCES

- <sup>1</sup> Bureau USC. Health and nutrition, Census Bureau Statistical Abstracts of the United States, Washington DC, U.S., 117 (2009).
- <sup>2</sup> M.N. Rahaman, D.E. Day, B.S. Bal, Q. Fu, S.B. Jung, L.F. Bonewald, and A. P. Tomsia, Bioactive Glass in Tissue Engineering, *Acta Biomater.*, **7**, 2355-73 (2011).
- <sup>3</sup> L.L. Hench, The Story of Bioglass®, *J. Mater. Sci. Mater. Med.*, **17**, 967-78 (2006).
- <sup>4</sup> T. S. Huang, M. N. Rahaman, N. D. Doiphode, M. C. Leu, B. S. Bal, D. E. Day, and X. Liu, Porous and Strong Bioactive Glass (13–93) Scaffolds Fabricated by Freeze Extrusion Technique, *Mater. Sci. Eng. C*, **31**, 1482-89 (2011).
- <sup>5</sup> A. M. Deliormanlı and M. N. Rahaman, Direct-write Assembly of Silicate and Borate Bioactive Glass Scaffolds for Bone Repair, *J. Eur. Ceram. Soc.*, **32**, 3637-46 (2012).
- <sup>6</sup> Q. Fu, E. Saiz, and A. P. Tomsia, Direct Ink Writing of Highly Porous and Strong Glass Scaffolds for Load-bearing Bone Defects Repair and Regeneration, *Acta Biomater.*, **7**, 3547-54 (2011).
- <sup>7</sup> Q. Fu, E. Saiz, M. N. Rahaman, and A. P. Tomsia, Bioactive Glass Scaffolds for Bone Tissue Engineering: State of the Art and Future Perspectives, *Mater. Sci. Eng. C*, **31**, 1245-56 (2011).
- <sup>8</sup> A. J. Wagoner Johnson and B. A. Herschler, A Review of the Mechanical Behavior of CaP and CaP/polymer Composites for Applications in Bone Replacement and Repair, *Acta Biomater.*, **7**, 16-30 (2011).
- <sup>9</sup> P. Miranda, A. Pajares, F. Guiberteau. Finite Element Modeling as a Tool for Predicting the Fracture Behavior of Robocast Scaffolds. *Acta Biomater*, **4**:1715-24 (2008)
- <sup>10</sup> C.B. Carter and M.G. Norton, *Ceramic Materials : Science and Engineering*, Springer, New York, NY (2007).
- <sup>11</sup> F. J. Martinez-Vazquez, F. H. Perera, P. Miranda, A. Pajares, and F. Guiberteau, Improving the Compressive Strength of Bioceramic Robocast Scaffolds by Polymer Infiltration, *Acta Biomater.*, **6**, 4361-8 (2010).

- <sup>12</sup> Y. Shanjani, Y. Hu, R. M. Pilliar, and E. Toyserkani, Mechanical Characteristics of Solid-Freeform-Fabricated Porous Calcium Polyphosphate Structures with Oriented Stacked Layers, *Acta Biomater.*, **7**, 1788-96 (2011).
- <sup>13</sup> P. Miranda, A. Pajares, E. Saiz, A. P. Tomsia, and F. Guiberteau, Mechanical Properties of Calcium Phosphate Scaffolds Fabricated by Robocasting, *J. Biomed. Mater. Res. A*, **85**, 218-27 (2008).
- <sup>14</sup> X. Liu, M. N. Rahaman, and Q. Fu, Bone Regeneration, Mineralization, and Mechanical Response of Bioactive Glass (13-93) Scaffolds with Oriented and Trabecular Microstructures Implanted in Rat Calvarial Defects., *Acta Biomater.*, in press (2012).
- <sup>15</sup> Q. Fu, M. N. Rahaman, B.S. Bal, L.F. Bonewald, K. Kuroki, R.F. Brown, Silicate, Borosilicate, and Borate Bioactive Glass Scaffolds with Controllable Degradation Rate for Bone Tissue Engineering Applications. I. In Vitro and In Vivo Biological Evaluation, *J. Biomed. Mater. Res. A*, **95**, 172-79 (2010).
- <sup>16</sup> Q. Fu, M. N. Rahaman, and D. E. Day, Accelerated Conversion of Silicate Bioactive Glass (13-93) to Hydroxyapatite in Aqueous Phosphate Solution Containing Polyanions, *J. Am. Ceram. Soc.*, **92**, 2870-76 (2009).
- <sup>17</sup> S. Radin, P. Ducheyne, S. Falaize, and A. Hammond, In Vitro Transformation of Bioactive Glass Granules into Ca-P Shells, *J. Biomed. Mater. Res.*, **49**, 264-72 (2000).
- <sup>18</sup> D. P. Byrne, D. Lacroix, J. A. Planell, D. J. Kelly, and P. J. Prendergast, Simulation of Tissue Differentiation in a Scaffold as a Function of Porosity, Young's modulus and Dissolution rate: Application of Mechanobiological Models in tissue engineering, *Biomaterials*, **28**, 5544-54 (2007).